

Two-photon photoemission spectromicroscopy of noble metal clusters on surfaces studied using time-of-flight photoemission electron microscopy

This article has been downloaded from IOPscience. Please scroll down to see the full text article.

2005 J. Phys.: Condens. Matter 17 S1319

(<http://iopscience.iop.org/0953-8984/17/16/003>)

View [the table of contents for this issue](#), or go to the [journal homepage](#) for more

Download details:

IP Address: 129.252.86.83

The article was downloaded on 27/05/2010 at 20:39

Please note that [terms and conditions apply](#).

Two-photon photoemission spectromicroscopy of noble metal clusters on surfaces studied using time-of-flight photoemission electron microscopy

Mirko Cinchetti and Gerd Schönhense

Johannes Gutenberg-Universität, Institut für Physik, 55099 Mainz, Germany

E-mail: cinchett@uni-mainz.de

Received 14 June 2004, in final form 9 December 2004

Published 8 April 2005

Online at stacks.iop.org/JPhysCM/17/S1319

Abstract

Time-of-flight two-photon photoemission spectromicroscopy was used to investigate Cu surface inhomogeneities and Ag cluster films deposited on a Si(111) substrate. Femtosecond laser radiation with wavelength around 400 nm (photon energy 3.1 eV) was used for excitation. The metal aggregates have linear dimensions in the range between 40 nm and several 100 nm. It is shown that the two-photon photoemission spectra of the Cu and Ag nanoclusters reveal the same qualitative differences from the spectra of the corresponding homogeneous and clean metal surfaces. In particular, they show an enhanced photoemission yield (up to 70 times higher) and present a different overall shape, characterized by differences around the Fermi level onset and a steeper intensity increase at lower final state energies. These differences are discussed in terms of the excitation of localized surface plasmons in the clusters and a resulting modification of the near-zone electromagnetic field, which in turn influences the two-photon photoemission and its dynamics. Moreover, it is shown that a positive unit charge (photohole) resides on the clusters during the timescale relevant for the two-photon photoemission process.

1. Introduction

Two-photon photoemission (2PPE) spectroscopy of metal surfaces using femtosecond lasers is widely used to obtain information about the unoccupied electronic states between the Fermi energy and the vacuum level and on their relaxation dynamics [1–5]. The combination of this technique with time-of-flight photoemission electron microscopy (TOF-PEEM) allows one to obtain additional lateral resolution on the recorded photoemission signal. Such a spectromicroscopic technique is particularly suitable for the analysis of structured samples.

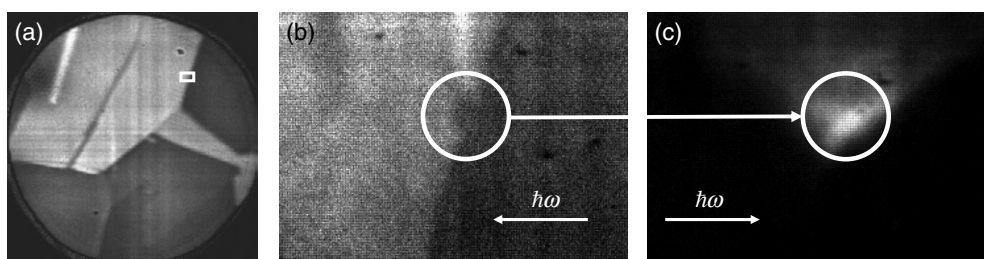


Figure 1. (a) A UV-PEEM image of a $500\ \mu\text{m}$ wide region of the polycrystalline copper sample taken with a deep-UV lamp as excitation source. Due to their different work functions, different crystallites appear with different grey levels. (b) A detailed image of the $10 \times 6\ \mu\text{m}^2$ region of interest marked in (a). (c) A fs laser PEEM image of the same region of the sample under s-polarized laser illumination (photon energy 3.3 eV). The 2PPE yield is strongly enhanced at the inhomogeneity marked with a circle. The arrows in (b) and (c) indicate the photon impact direction.

The first results obtained with the so-called 2PPE TOF-PEEM spectromicroscopy were presented in [6]. The 2PPE spectra from Cu surface inhomogeneities present on a clean Cu polycrystalline sample have been compared to those measured from homogeneous Cu surface regions. In [7], we compared the 2PPE spectra from Ag nanoparticle films deposited on Si(111) to those of a 100 nm thick Ag layer. In both cases, the noble metal clusters studied had linear dimensions ranging between 40 nm and several 100 nm.

In this paper we show that the 2PPE spectra from granular films (nanocluster aggregates) and isolated nanoclusters reveal the same qualitative differences from the corresponding homogeneous surfaces, showing 2PPE spectra as known from the literature [8, 3]. In the following, we will refer to the latter 2PPE spectra as the *reference spectra*. In particular, we focus our attention on the enhancement of the 2PPE yield of the nanoclusters and on the overall shape of their 2PPE spectra. The latter are characterized by differences around the Fermi level onset and by a steeper intensity increase at lower final state energies, if compared to their reference spectra. The key role for the interpretation of the observed behaviour is played by the excitation of localized surface plasmons (LSP) in the clusters and the resulting modification of the near-zone (NZ) electromagnetic field. The collective response of the conduction electrons strongly influences the 2PPE and its dynamics.

2. Experimental set-up

The experiments have been performed in UHV. The procedure of preparation of the polycrystalline Cu sample was described in [6]. Crystallites with different surface orientations have different work functions, ranging between 4.6 eV for Cu(112) and 5.0 eV for Cu(111). Illuminating the sample with a deep-UV lamp (photon energy cut-off at 5.8 eV), electrons are emitted by one-photon photoemission (1PPE). Since the total 1PPE yield depends on the work function, and thus on the surface orientation, different crystallites show up in the PEEM image as different grey levels. An example is shown in figure 1(a), where different Cu crystallites present on a $500\ \mu\text{m}$ wide region of the Cu sample are clearly visible.

The Ag sample consists of Ag nanoparticle films with nominal thickness varying from 0 to 20 nm, and of a continuous layer (100 nm nominal thickness). They were deposited by electron beam evaporation onto a Si(111) substrate at room temperature with a coverage profile of a stepped wedge. The Si(111) surface was prepared by sputtering and heating cycles for removal of the native oxide and characterized by LEED. The structure of the deposited

films was investigated *ex situ* by atomic force microscopy. The Ag nanoparticle films consist of nanoparticles with average linear dimensions increasing with increasing Ag coverage, and varying between 40 and 80 nm. In this paper we will consider a film with a Ag mass thickness of 5 nm, consisting of Ag nanoparticles with average linear dimensions of 50 nm and covering approximately 20% of the Si substrate (labelled as region 3 in [7]). It will be referred to as *the Ag nanoparticle film*. The sample preparation and characterization are described in detail in [7]. High-resolution TEM investigations [9] revealed that the deposited nanoparticles are mostly multiply twinned crystallites with (111)-oriented facets. After preparation and characterization the sample was transferred through air to the TOF-PEEM chamber.

The fundamental of a femtosecond Ti:sapphire laser (wavelength tunable between 750 and 850 nm, repetition rate 80 MHz) was frequency doubled by a commercial device, giving a photon energy tunable between 2.9 and 3.3 eV and a pulse width <200 fs. The frequency-doubled beam was focused on the samples at an angle of 65° with respect to the surface normal, obtaining a fluence of $6.4 \mu\text{J cm}^{-2}$. A Fresnel rhomb allowed us to change the direction of the polarization vector. A Hg deep-UV lamp served as illumination source for the 1PPE. The TOF-PEEM was a modified commercial PEEM equipped with a drift tube and a delay line detector; details can be found in [6, 7, 10, 11].

3. Results

3.1. Cu surface inhomogeneities

Figure 1(b) shows a PEEM image of the $10 \times 6 \mu\text{m}^2$ region of interest marked in figure 1(a) with a rectangle. The image was obtained by illuminating the sample with the deep-UV lamp. The stripes in (a) and the raster in (b) and (c) that are also visible in figure 4 are artefacts due to the adjustment of the TOF-PEEM electronics. Figure 1(c) shows a PEEM image of the same region of the Cu sample, illuminated with s-polarized laser light with a photon energy of $\hbar\omega = 3.3$ eV. Although (b) and (c) are taken at identical sample positions, the images look completely different. The laser-excited image shows a bright spot at a position that appears dark in the UV-PEEM image (b). The bright spot in (c) exhibits a caustic-like feature. The comparison makes it clear that the 2PPE yield is enhanced in the centre of figure 1(c). According to (b) this area corresponds to a surface inhomogeneity at the border between two copper crystallites with different orientations, marked with a circle. The apparent linear dimension of this inhomogeneity is approximately 400 nm. It should be noted, however, that the apparent sizes of 3D objects on surfaces can be considerably influenced by electron optical artefacts in PEEM [12]. In particular, protruding objects give rise to deformations of the homogeneous extractor field that, in turn, can lead to an increase of the image size of the 3D object. Also, caustic-like features can be caused by the local field deformation.

Figure 2 shows a typical 2PPE spectrum of such a surface inhomogeneity (dashed curve) compared to its reference spectrum (continuous curve), taken from a homogeneous region of a Cu crystallite. The energy scale is referred to the Fermi level. The spectra are plotted in their original intensity scale, normalized to equal lateral area on the surface. Moreover, they have been normalized with the PEEM transmission function ($\propto E_k^{-1}$, where E_k is the electron kinetic energy). It takes into account that electrons with different starting kinetic energies at the sample surface have different probabilities of travelling through the electron optical column and being eventually recorded.

In the inset the behaviour of the spectra at the Fermi level onset (appearing at a final state energy of about $2\hbar\omega = 6.6$ eV for the reference spectrum) is shown. Here, the reference spectrum has been expanded by a factor of 4.

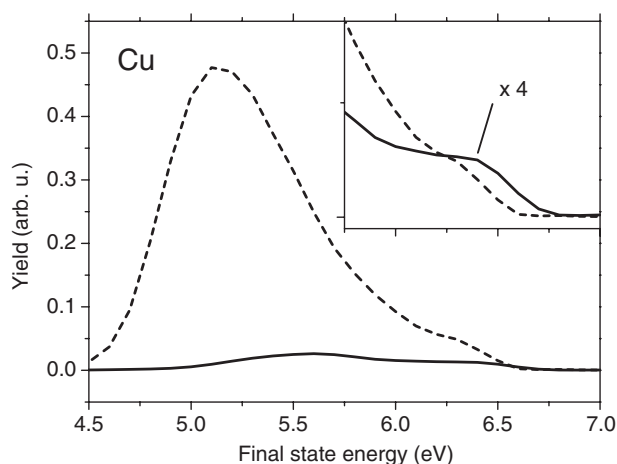


Figure 2. Dashed curve: a typical 2PPE spectrum of a Cu surface inhomogeneity like the one shown in figure 1(c). Continuous curve: the 2PPE reference spectrum of a homogeneous region of the Cu sample with the same lateral size. 2PPE was induced by s-polarized laser light with photon energy $\hbar\omega = 3.3$ eV. Inset: the behaviour of the spectra at the 2PPE Fermi level onset. The reference spectrum has been expanded by a factor of 4.

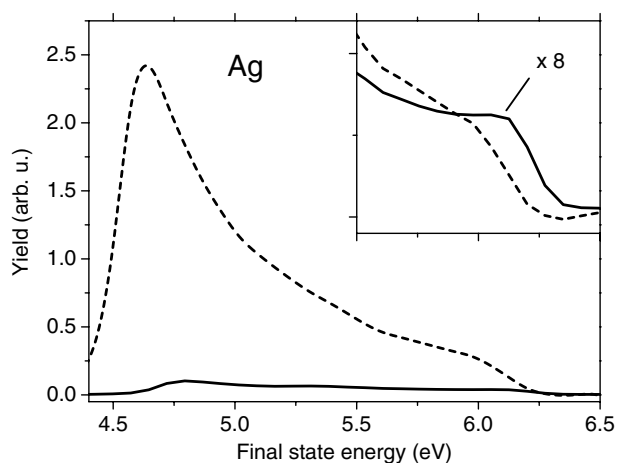


Figure 3. Dashed curve: the 2PPE spectrum of the Ag nanoparticle film (nanoparticle average size: ≈ 50 nm). Continuous curve: the 2PPE reference spectrum of the 100 nm thick Ag film. 2PPE was induced by p-polarized laser light with photon energy $\hbar\omega = 3.1$ eV. Inset: the behaviour of the spectra at the Fermi level onset (appearing at a final state energy of about $2\hbar\omega = 6.2$ eV) is shown. Here, the reference spectrum has been scaled by a factor of 8.

3.2. Ag nanoparticle film

Figure 3 compares the 2PPE spectra of the Ag nanoparticle film with mass thickness 5 nm (dashed curve) to its reference spectrum (continuous curve), taken from the 100 nm thick Ag film. Like in figure 2, the spectra are plotted on their original intensity scale, normalized to equal lateral surface area and corrected with the PEEM transmission function. 2PPE was induced by p-polarized laser light with photon energy $\hbar\omega = 3.1$ eV. In the inset the behaviour of the spectra at the Fermi level onset (appearing at a final state energy of about $2\hbar\omega = 6.2$ eV) is shown. Here, the reference spectrum has been scaled by a factor of 8.

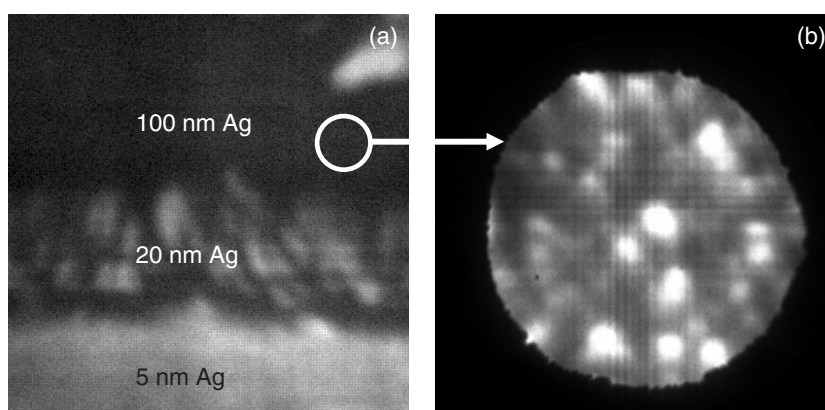


Figure 4. (a) A fs laser PEEM image of the nominally 5 and 20 nm thick Ag cluster films and the 100 nm thick Ag film (field of view $45 \mu\text{m}$). (b) A PEEM image of the $4 \mu\text{m}$ diameter region of the 100 nm thick film marked in (a) with a circle. Both images are taken with illumination with s-polarized laser light ($h\nu = 3.0 \text{ eV}$). Ag surface inhomogeneities are clearly visible in the detailed image. In (b), the contrast and brightness have been enhanced to make the structures visible.

Table 1. 2PPE yield enhancement close to the Fermi level onset E_F , at the maximum yield Y_{max} of the 2PPE spectra and the total yield (area below the spectra) of Cu and Ag clusters compared to the corresponding reference spectra.

	Enhancement at E_F	Enhancement at Y_{max}	Total enhancement
Cu	4	20	16
Ag	8	80	70

4. Discussion

A comparison between figures 2 and 3 makes it clear that the 2PPE spectra from the Cu and Ag clusters show the same qualitative differences from the corresponding reference spectra.

- (i) First of all, they are characterized by a strongly enhanced 2PPE total yield (areas below the spectra). The enhancement factor is about 16 for the Cu cluster, and about 70 for the Ag nanoclusters.
- (ii) Second, the Fermi level onset of the cluster spectra is shifted by 0.12 and 0.13 eV towards lower final state energies for Cu and Ag, respectively.
- (iii) Third, the cluster spectra exhibit a much steeper increase of the photoemission intensity towards lower final state energies. To quantify this statement, we evaluated the 2PPE yield enhancement close to the Fermi level onset E_F and close to the maximum yield Y_{max} of the 2PPE spectra. The results are shown in table 1.

Points (i)–(iii) are discussed in sections 4.1–4.3, respectively.

4.1. Total 2PPE yield

According to the three-step model of photoemission [13], the experimentally measured electron energy spectrum in the threshold region is given by the product of three factors: the two-photon excitation probability yielding the initial (nascent) electron distribution function $P(E, \omega)$, the electron transport function and the electron escape function $T(E)$, describing the transmission through the surface to vacuum.

In the narrow range of electron energies considered here ($\Delta E \approx 2$ eV), the electron transport function in a cluster and that in the corresponding smooth metal surface can be assumed to be identical. Thus, the enhancement of the 2PPE yield G from a noble metal cluster (C) with respect to the yield from the corresponding smooth metal surface (S) can be written as

$$G = \frac{Y_C}{Y_S} \approx \frac{T_C}{T_S} \frac{P_C}{P_S} \quad (1)$$

where the distribution and transmission probabilities P and T are obtained from the respective functions $P(E)$ and $T(E)$ by integration over the interval ΔE .

Let us derive a rough estimate for the value of the ratio T_C/T_S . To do so, we consider the enhancement of the 1PPE yield from a noble metal cluster (C) with respect to the 1PPE yield from the corresponding smooth surface. If 1PPE is excited with a deep-UV lamp, whose energy cut-off lies far away from the LSP excitation energy in Ag and Cu clusters, we can assume to a good approximation equal excitation probabilities in equation (1). In fact, if no LSP excitation occurs, the 1PPE excitation probabilities in metal clusters and smooth metal surfaces should be approximately the same for our system. This is true if the band structure in the metal cluster does not significantly differ from the bulk. For the given sizes of about 50 nm the ‘small solid approach’ is still a good approximation. Confinement effects will thus not influence the photoexcitation step significantly. Surface states could, in principle, play a role. In our sample these are quenched due to oxygen coverage from the *ex situ* preparation. Within this approximation, the ratio T_C/T_S is equal to the 1PPE yield enhancement. The latter quantity can be determined using UV-PEEM images [14]. The measured intensity difference of 0.75 is multiplied by the inverse coverage ratio, giving a value of $T_C/T_S \approx 3$. Owing to the surface curvature of spherical or hemispherical particles, electrons can escape from a larger solid angle interval than for smooth surfaces, where threshold photoemission is restricted by the escape cone.

In addition, metal clusters are characterized by a lower work function (in our samples 0.5 eV for Cu and 0.1 eV for Ag) than the corresponding homogeneous surface. This is included in the experimental value of T_C/T_S . Obviously, the observed values of G (70 and 16 for Ag and Cu, respectively) cannot be explained by the fact that $T_C/T_S > 1$ alone.

The key role in the explanation of the measured values for G is played in equation (1) by the high values assumed by the ratio P_C/P_S . Shalaev *et al* [15] calculated this quantity for Ag cluster films by assuming them to be small polarizable elements of a self-affine fractal. They show that in smooth films the dominant contribution to the two-photon excitation probability is given by direct, i.e. k -conserving two-photon transitions. On the other hand, in a Ag cluster fractal film excited with photons whose energy range lies close to the LSP resonance, the most important contribution to P_C comes from indirect (i.e. non- k -conserving) transitions arising due to the missing translational symmetry. According to [15] these transitions are induced by the strong spatial dependence (leading term $\propto r^{-3}$, where r is the distance from the centre of the cluster) of the NZ fields associated with the LSPs. These high NZ fields come along with an enhanced electron emission which can also be interpreted as a non-radiative decay of the LSP into a one-electron excitation.

The theoretical value of the LSP resonance in Ag spherical particles (in the large particle limit) in vacuum is $\hbar\omega_{\text{LSP}}(\text{Ag}) = 3.5$ eV [16]. For Ag nanoparticle films on SiO₂, extinction curves with maxima shifting from 3.4 to 3.0 eV with increasing coverage have been measured [17, 18]. Since the resonance curves have a width of about 0.7 eV, our photon energy of 3.1 eV lies within the region of enhanced extinction due to the vicinity of the LSP resonance. In this region a strong enhancement of the 2PPE yield has been previously observed, for example in [4].

For excitation frequencies close to ω_{LSP} Stuckless *et al* [19] reported values for G of the order of 10^3 . In our case, the apparently smaller enhancement factor could be due to the fact that the 100 nm thick film used as reference for the 2PPE yield from a smooth film is not completely homogeneous. This is indeed confirmed by figure 4(b) which shows the PEEM image of a $4 \mu\text{m}$ region of the 100 nm thick Ag film illuminated by s-polarized laser light ($\hbar\omega = 3.0 \text{ eV}$). Ag surface inhomogeneities with apparent linear dimensions varying between 200 and 400 nm are clearly visible, and show a strongly enhanced 2PPE yield as compared with the background intensity. Obviously, the 100 nm thick Ag film is not smooth, but exhibits surface inhomogeneities. Consequently the yield of the reference spectra is already enhanced by LSP excitation.

The excitation of LSP plays a role also for the measured 2PPE yield enhancement in Cu clusters. There is, however, an important difference between this case and the above-discussed NZ field enhancement in the Ag nanoparticle films. In fact, we are dealing in figure 1 with an *isolated* cluster or inhomogeneity.

First of all we observe that in the case of isolated clusters, the polarization of the incoming light plays an important role. Depending on the cluster's shape, an enhancement of the 2PPE yield may be selectively achieved only with a particular laser polarization. For example in oblate spheroids, the LSP resonance splits into two modes [20]: the (1, 1) mode with the dipole along the main axis and the (1, 0) mode with it along the short axis. If the spheroid lies on the surface with the short axis directed along the surface normal, p-polarized light excites both modes, since the electric field has a component along both axes. On the other hand, s-polarized light may excite only the (1, 1) mode. This selective excitation is not observable in the Ag nanoparticle films, since they basically consist of randomly oriented nanoclusters. This is confirmed by the fact that the PEEM images of the Ag sample have the same qualitative behaviour for s and p polarization. A detailed analysis of the 2PPE spectral dependence on the laser polarization will be discussed in a separate paper.

An interesting quantity for this situation is the absorption efficiency Q_{abs} . We recall that, by definition, $Q_{\text{abs}} > 1$ implies that the distortion of the incoming plane wave at the small metal particle surface results in the absorption of all photons from an increased *effective* particle cross-section [21]. For a Cu spherical particle with $R = 100 \text{ nm}$ immersed in water, $Q_{\text{abs}}(\hbar\omega = 3.1 \text{ eV}) \approx 1.6$ [21]. Note that $Q_{\text{abs}} > 1$ even away from the LSP resonance.

The resonance of LSP in Cu spherical particles in vacuum occurs at $\hbar\omega_{\text{LSP}}(\text{Cu}) = 2.1 \text{ eV}$ [20]. This value is quite far from the photon energy used, $\hbar\omega = 3.3 \text{ eV}$. This explains why the 2PPE yield enhancement relative to the reference spectrum is less pronounced in the Cu clusters than in the Ag cluster film. Moreover, extinction spectra show that Ag spheres in vacuum have a better developed LSP resonance than Cu. This is a consequence of the small imaginary part of the dielectric function of Ag in the resonance region.

The above considerations suggest that even if *LSP are not excited* in the Cu clusters, but the laser frequency is in a region where the *absorption efficiency* of the particle is larger than one, the photoemission yield is still enhanced. This is due to the fact that synchronous excitations of the electrons in the metal particle induced by the laser [22] enhance the NZ fields. This affects the 2PPE yield in the same qualitative way as the resonant excitation of LSP. The difference between these two situations is that in the case of LSP excitation, the frequency of the electron oscillation corresponds to a natural mode of the system: the field enhancement in this case is much stronger.

4.2. Shift of the Fermi level onset

Let us now discuss the respective shifts of 0.13 and 0.12 eV of the Fermi level onset in the Cu and Ag cluster spectra towards lower final state energies in comparison with those of the

corresponding reference spectra (see the insets in figures 2 and 3). The shifts can be explained using the *final state cluster charge model* of Wertheim *et al* [23, 24].

During the photoemission process a unit positive charge can remain localized on a nanoparticle supported by a poorly conducting substrate such as carbon or a semiconductor. In this case charge neutralization happens on a timescale longer than the intrinsic timescale of photoemission but long before the next process of photoemission from the given particle. Given our experimental conditions, a nanoparticle cannot emit more than one photoelectron per laser pulse. This is evident from the total yield values and the experimental count rate [6, 7]. Thus there is no long-term charge build-up like on insulators. Instead, a transient state with one positive charge located on the surface of the particle exists. The Coulomb energy of this transient, non-neutralized state of the particle leads to a corresponding reduction of the final state energy of the outgoing photoelectron, fulfilling the energy balance equation of photoemission. The resulting shift of the Fermi level onset in the spectra (ΔE_F) depends on the characteristic time τ_n for the positive charge neutralization [25]. In the limit $\tau_n \rightarrow \infty$ the shift is $\Delta E_F \sim e^2/R$ for spherical metal clusters.

Using the measured shift value of approximately 0.1 eV, we obtain a rough estimate for the particle radius $R \approx 15 \pm 10$ nm. Within the experimental error we can consider this explanation valid for the Ag cluster film. It may also cause the shift of the low-energy cut-off.

The Cu hot spot appears an order of magnitude larger in the images. However, we have mentioned the problem of the apparent size. In addition, the shape of the Cu cluster could deviate strongly from a spherical shape. Possibly, prolate nanostructures protruding from the surface could exhibit the final state unit charge effect even if one end of the structure is connected with the underlying metal.

4.3. Different overall shapes of the spectra

The different overall shapes of the Cu and Ag cluster spectra with respect to the corresponding reference spectra give information about the different dynamics of 2PPE in the small metal particles with respect to the homogeneous metal surfaces. We recall that the Cu and Ag cluster spectra are characterized by a much steeper increase of the 2PPE yield at low final state energies (close to Y_{\max}) than the corresponding reference spectra.

The description of two-photon excitation as a two-step process, where a first (pump) photon creates a non-equilibrium distribution which is probed by a second (probe) photon, is justified whenever the sum frequency ω' of the two photons is far away from ω_{LSP} [26]. At our experimental conditions ($\hbar\omega' \approx 6$ eV) this is always the case, since $\hbar\omega_{\text{LSP}}$ for Ag and Cu nanoparticles lies between 2 and 4 eV. We now use this illustrative picture to describe the dynamics of a 2PPE process in Cu and Ag homogeneous surfaces and in the corresponding clusters.

4.3.1. Homogeneous Cu and Ag surfaces. In our experiments, the photon momentum of the incident light q is negligible with respect to the electron momentum k . In fact for $\hbar\omega' \approx 6$ eV one has $q \approx 3 \times 10^5 \text{ cm}^{-1} \ll k_F$, where k_F is the momentum of electrons at the Fermi level that is of the order of 10^8 cm^{-1} for most metals. This implies that photoemission is dominated by direct transitions ($\Delta k = 0$). An inspection of the Cu and Ag band structure [13] makes it clear that (at our photon energies) direct 2PPE transitions can only proceed through virtual states [15]. Thus, only simultaneous excitations are possible. In simultaneous 2PPE transitions there is no time delay between the absorption of two photons: this means that the probe photon is absorbed from the nascent non-thermal distribution produced by the absorption of the pump photon from the laser field.

4.3.2. Cu and Ag clusters. In Cu and Ag clusters, the pump and probe photon are absorbed out of the enhanced NZ field of the particle (or a neighbouring one), or result directly from the decay of the collective mode into a single electron–hole pair. The strong spatial dependence of the NZ fields allows 2PPE to proceed via indirect transitions ($\Delta k \neq 0$) through real states as well [15]. Thus, both simultaneous and cascade (sequential) excitations are possible. In a sequential excitation, the intermediate state population experiences an energy-dependent relaxation process (mainly due to electron–electron scattering [1, 3]) with lifetimes ranging from about 2 fs [3] at its high-energy end to several hundreds of femtoseconds close to E_F . Note that the term population refers to the statistical average of many single-electron excitations and not to an ensemble in one particle. The probe photon is then absorbed within the width of the laser pulse (~ 200 fs). The energy-dependent relaxation of the intermediate state population during this intrinsic time delay causes a stronger reduction of the 2PPE yield at higher energies than at lower energies. This explains the difference in shape of the spectra. Two quantitative facts are important: first, the high photoabsorption cross-section of the collective modes causes a high concentration of electromagnetic energy in the nanoparticle. A resonantly excited free Ag cluster absorbs of the order of 100 photons per laser pulse at our experimental conditions. Second, the partly thermalized ‘hot electrons’ in the intermediate state are trapped for some time in the nanoparticle. Their diffusion into the substrate is hampered by the poorly conducting contact to the surface; cf section 4.2. The required time for full thermalization of the electron gas exceeds the width of our laser pulse [27].

5. Conclusions and outlook

Time-of-flight photoemission spectromicroscopy was used to compare the two-photon photoemission spectra of Cu and Ag clusters with linear dimensions ranging between 40 nm and several 100 nm to those of the corresponding homogeneous surfaces. The former spectra are characterized by an enhanced total 2PPE yield, by a shift (≈ 0.1 eV) of the Fermi level onset towards lower final state energies and by a much steeper increase of the 2PPE yield towards lower final state energies.

The shift of the Fermi level onset in the cluster spectra has been explained by assuming that a positive unit charge may reside on the clusters [23] during the timescale relevant for the 2PPE process. On the other hand, we have shown that the total 2PPE yield enhancement and the different overall shape of the spectra can be explained by considering that the fs laser frequency was close to the LSP resonance of Ag nanoparticles (yield enhancement factor 70) and still in a region of strong collective response for Cu particles (factor 16). In fact, the synchronous oscillations induced by the laser in the metal electrons strongly enhance the electromagnetic energy density and the NZ field. Both play an important role in explaining the 2PPE spectra. The spatial dependence discussed by Shalaev *et al* [15] ($\propto r^{-3}$) is valid only in the case of a fractal aggregate. Clearly, the NZ field produced by isolated clusters strongly depends on their shape and orientation. It is responsible for the 2PPE enhancement and it affects the photoemission and its dynamics. In particular, the strong spatial dependence of the NZ fields allows indirect transitions through real intermediate states to take place in the metal clusters. Such transitions are forbidden or at least much less probable on homogeneous surfaces.

Further studies of nanoparticles with a known NZ field behaviour are being performed, in order to find a quantitative dependence between 2PPE and the NZ field behaviour.

Acknowledgments

Excellent cooperation with A Oelsner, A Gloskovskii, S A Nepijko, G H Fecher and H J Elmers (University of Mainz) and a fruitful discussion with K Horn (Fritz-Haber-Institute, Berlin) are

gratefully acknowledged. The work was funded by BMBF (03N6500) and Stiftung Rheinland-Pfalz für Innovation (project 535).

References

- [1] Knoesel E, Hotzel A, Hertel T, Wolf M and Ertl G 1996 *Surf. Sci.* **368** 76
- [2] Petek H and Ogawa S 1997 *Prog. Surf. Sci.* **56** 239
- [3] Bauer M and Aeschlimann M 2002 *J. Electron Spectrosc. Relat. Phenom.* **124** 225
- [4] Lehmann J, Merschdorf M, Pfeiffer W, Thon A, Voll S and Gerber G 2000 *Phys. Rev. Lett.* **85** 2921
- [5] Shumay I L, Höfer U, Reuß C, Thomann U, Wallauer W and Fauster T 1998 *Phys. Rev. B* **58** 13974
- [6] Cinchetti M, Oelsner A, Fecher G H, Elmers H J and Schönhense G 2003 *Appl. Phys. Lett.* **83** 1503
- [7] Cinchetti M, Valdaitsev D A, Gloskovskii A, Oelsner A, Nepijko S A and Schönhense G 2004 *J. Electron Spectrosc. Relat. Phenom.* **137–140** 249
- [8] Ogawa S and Petek H 1996 *Surf. Sci.* **363** 313
- [9] Gloskovskii A *et al* 2005 at press
- [10] www.focus-gmbh.com
- [11] Schönhense G, Oelsner O, Schmidt O, Fecher G H, Mergel V, Jagutzki O and Schmidt-Böcking H 2001 *Surf. Sci.* **480** 180
- [12] Nepijko S A, Sedov N N, Schmidt O, Fecher G H and Schönhense G 2002 *Ann. Phys., Lpz.* **11** 39
- [13] Berglund C N and Spicer W E 1964 *Phys. Rev. A* **136** 1030
- [14] Cinchetti M 2004 *PhD Thesis* University of Mainz
- [15] Shalaev V M, Douketis C, Haslett T, Stuckless T and Moskovits M 1996 *Phys. Rev. B* **53** 11193
- [16] Liebsch A 1993 *Phys. Rev. B* **48** 11317
- [17] Kreibig U and Genzel L 1985 *Surf. Sci.* **156** 678
- [18] Hoevel H, Fritzt S, Hilger A, Kreibig U and Vollmer M 1993 *Phys. Rev. B* **48** 18178
- [19] Stuckless J T and Moskovits M 1989 *Phys. Rev. B* **40** 9997
- [20] Kreibig U and Vollmer M 1993 *Optical Properties of Metal Clusters (Springer Series in Materials Science)* (Berlin: Springer)
- [21] Messinger B J, Ulrich von Raben K, Chang R K and Barber P W 1981 *Phys. Rev. B* **24** 649
- [22] Stratton J A 1941 *Electromagnetic Theory* (New York: McGraw-Hill)
- [23] Wertheim G K, Di Cenzo S B and Youngquist S E 1983 *Phys. Rev. Lett.* **51** 2310
- [24] Wertheim G K and Di Cenzo S B 1988 *Phys. Rev. B* **37** 844
- [25] Hövel H, Grimm B, Pollmann M and Reihl B 1998 *Phys. Rev. Lett.* **81** 4608
- [26] Timm C and Bennemann K H 2004 *J. Phys.: Condens. Matter* **16** 661
- [27] Rethfeld B, Kaiser A, Vicanek M and Simon G 2002 *Phys. Rev. B* **65** 214303